The Content of Different Hydrogen Bond Models and Crystal Structure of Eucalyptus Fibers during Beating

Longting Yuan,[a,b] Jinquan Wan,[b,c,]* Yongwen Ma,[b,c] Yan Wang,[b,c] Mingzhi Huang,[b,c] and Yangmei Chen [d]

Different hydrogen bond and crystalline cellulose structure models of eucalyptus fibers were studied by Fourier transform infrared spectrometer (FTIR), X-ray diffraction (XRD), and Cross-Polarization Magic Angle Spinning Carbon-13 Nuclear Magnetic Resonance (CP/MAS ^{13}C NMR). It was shown that when the beating time was increased from 5 to 15 min., the content of inter-molecular hydrogen bonds, O(6)H···O3′, increased by 11.2% as measured by FTIR. However, the content of the inter-molecular hydrogen bonds decreased quickly as the beating time was increased from 15 to 25 min. Meanwhile, the contents of the intra-molecular hydrogen bond, O(2)H···O(6) and O(3)H···O(5), changed from 8.25% to 8.18% and from 39.33% to 31.27%, respectively, when the beating time increased from 5 to 15 min. The content of the intra-molecular hydrogen bonds increased quickly with the further increase in the beating time. It was shown by XRD that there was a little difference in the average width of crystallite size in the (002) lattice plane when the beaten time was between 5 to 25 min. Non-linear fitting of the cellulose C4 region of the ^{13}C CP/MAS NMR showed that the average lateral fibril aggregate dimensions and the content of different cellulose polymorphs changed during beating.

Keywords: Eucalyptus fibers; Beating; Hydrogen bond; Crystal structure

Contact information: a: School of Light Chemical and Food Science Engineering, South China University of Technology, Guangzhou 510640, PR China; b: State Key Laboratory of Pulping and Papermaking Engineering, South China University of Technology, Guangzhou 510640, PR China; c: School of Environmental Science and Engineering, South China University of Technology, Guangzhou 510006, PR China; d: Tianjin Key Laboratory of Pulp and Paper, College of Materials Science and Chemical Engineering, Tianjin University of Science and Technology, Tianjin 300457, PR China;
** Corresponding author: ppjqwan@scut.edu.cn.*

INTRODUCTION

It is well known that wood is an abundant, a renewable, and a biodegradable composite with many useful applications, such as papermaking, building and furniture construction, and as a natural reinforcement aid in polymer composites (Jiménez *et al.* 2006; Baratieri *et al.* 2008; Lorenzo *et al.* 2009); however, tropical deforestation is an expanding global issue (Sodhi *et al.* 2010; Zhai *et al.* 2012); thus recycled cellulose has become a significant fiber source (up to 70%) for papermaking at the end of the 21st century (Wan and Ma 2004). So, it is very important to study the properties of cellulose fiber and find methods to improve recycled cellulose fiber properties. At present, most chemical and biological methods that improve the quality of the fiber can increase papermaking costs and can have environmental related issues (Blomstedt and Vuorimen 2007; Cao and Tan 2004; Pala *et al.* 2001). There are many changes of the characteristic

of cellulose fiber significantly formed into a wet web of paper when cellulose fiber is subjected to such processes as pressing, drying, printing, storage, and deinking. In order to find more effective ways for addressing the above mentioned problems and efficiency limitations with unbleached kraft pulps, this study investigated an approach of beating to modify eucalyptus fibers.

Plant cellulose fibers have complex composite structures that are mainly composed of cellulose, lignin, and hemicelluloses (Liu *et al*. 2008). Cellulose is the most common component found in the cell walls of higher plants. Typically, it is a high molecular weight linear polymer composed of *β*-D-glucopyranose units linked by (1→4)-glycosidic bonds. It is the nature of this polymer to form a long, flat polymer chain that exposes a number of hydroxyl groups and hydroxyl bonding sites, allowing the polymer chain to form a large amount of hydrogen bonds, leading to a crystalline structure (Gümüskaya *et al.* 2003). Native cellulose is known to be a composite of two distinct crystal types, namely I_α and I_β, whose fractions vary depending on the origin of the cellulose sample (Duchesne *et al.* 2001; Hult *et al.* 2003). Several studies have been undertaken to investigate the nature of the changes in cellulose superstructure. Crystallinity has an important effect on the physical, mechanical, and chemical properties of cellulose. For example, with increasing crystallinity, the tensile strength and dimensional stability decrease, while properties such as chemical reactivity and swelling decrease (Chen *et al.* 2010). As is well known, several techniques have been developed for determining the cellulose crystallinity and fibril aggregate dimensions, which include X-ray diffraction (XRD), solid-state ^{13}C nuclear magnetic resonance (^{13}C NMR) (Park *et al.* 2010; Miyamoto *et al.* 2011; Hult *et al.* 2002), and Fourier transform infrared spectroscopy (FTIR) (Mohkami and Talaeipour 2011; Liu *et al.* 2005). Furthermore, the hydrogen bonding network of cellulose has been studied with the application of infrared spectroscopy, and the hydrogen bonding region of the infrared absorptions has been almost completely assigned (Li *et al.* 2009; Maréchal and Chanzy 2000). Similarly, some authors have used Fourier transform infrared spectroscopy (FTIR) analysis to characterize the different hydrogen bond models of cellulose crystallinity. They concluded that the intra-molecular hydrogen bonds for O(2)H···O(6) and O(3)H···O(5), and the inter-molecular hydrogen bonds for O(6)H···O(3′) in cellulose I appear at 3455–3410 cm^{-1}, 3375–3340 cm^{-1}, and 3310–3230 cm^{-1}, respectively (Oh *et al.* 2005; Popescu *et al.* 2009). However, the content of the hydrogen bond and the details about the eucalyptus cellulose allomorphs during beating were not reported.

Eucalyptus pulps contain short fibers that are easily beaten. Beating is the most important physical treatment carried out on pulp before papermaking; it highly affects the physical properties of the paper and might be considered to be the first step in their "activation". It increases the area of contact between the fibers by increasing their surface area through fibrillation and by increasing their flexibility. For instance, the effect of beating on the changes of recycled eucalyptus fibers in morphological parameters, properties, crystal structure of cellulose, and pore structure of cellulose fiber were analyzed using FTIR and low-temperature nitrogen absorption by Chen *et al.* (2012). Ruel *et al.* (1978) used transmission electron microscopy (TEM) and scanning transmission electron microscopy (STEM) to study the structure of cellulose fibers. It is clear that any treatment of the wood material that removes constituents by breaking covalent bonds, as in chemical pulping, or by breaking physical bonds, as in mechanical treatments, will induce more or less modifications in the morphology (Kure and

Dahlqvist 1998) and the super-molecular organization of the fiber wall (Duchesne 2001; Billosta *et al.* 2006). These alterations may have a positive or negative effect on the fiber properties. Ibrahem *et al.* (1989) also studied the relation between fiber crystallinity and the properties of paper during beating. However, very little research has been carried out on the super-structure, especially regarding different hydrogen bonds of various cellulose crystalline types. Accordingly, it is important to study the super-structural changes in the eucalyptus fibers, with the broader aim at determining the content of different cellulose polymorphs during beating.

The goal of the present study was to analyze the ultra-structure of eucalyptus fibers and to illustrate the existence of hydrogen-bond in greater detail through the CP/MAS ^{13}C NMR analysis of cellulose in conjunction with X-ray diffraction and infrared spectrometry measurements using PeakFit software. The results of this investigation provided reliable data through peak-fitting analyses (Chen *et al.* 2004). The broader objectives of this work were to assess the contribution of beating to cellulose super-structural changes.

EXPERIMENTAL

Materials

Eucalyptus wood chips were cooked in autoclaves according to the conventional kraft process under the following conditions: 17% NaOH and 5% Na_2S, wood-to-liquor of 1:4, time-to-temperature of 2 h, cooking temperature of 170ºC, and time at cooking temperature of 2 h. The moisture content of unbleached wet eucalyptus pulp was 82.79% by weight in the never-dried state.

Methods

PFI beating and papermaking

PFI beating was carried out in accordance to TAPPI Test Method T248 wd-97 with the following conditions: pulp consistency 10%, bedplate-roll gap of 0.3 mm, bedplate speed 1400 r/min., and roll speed 1460 r/min. Different times were recorded. Handsheets were made on a Rapid-Köthen Sheet Former in accordance to TAPPI standards. The grammage of the unbleached eucalyptus handsheets was 60 g/m^2. Some handsheets were placed in a humidity-controlled room in accordance to TAPPI Test Method T402 and tested for physical properties 24 h later. Other handsheets were soaked in deionized water for at least 8 h. The rewetted handsheets were then disintegrated for 5000 revolutions in a laboratory disintegrator. Then the repulped fibers were remade into handsheets and dried accordingly to the described procedure above.

Fourier transform infrared spectrophotometer (FTIR)

The powdered cellulose and subsequently dried KBr were sifted through a 200-mesh screen. Cellulose (3.5 to 4.0 mg) and KBr (350 mg) were placed in an agate mortar, well-mixed and pulverized. The mixture was dried at 60ºC for 4 h and then poured into a tabletting mold to form transparent tablets. Spectra were recorded using a Bruker Vector 33 Fourier Transform Infrared Spectrophotometer (FTIR) set at a resolution of 4 cm^{-1} over the range 4000-400 cm^{-1}. For a better understanding of the structure of the samples, deconvolution of the spectra was carried out by using PeakFit software in combination

with Gaussian distribution function (Marechal *et al.* 2000; Oh *et al.* 2005; Popescu *et al.* 2009). The correlation values of the deconvolutions fitting was $r^2 \geqslant 0.99$; therefore, the use of this function is a good approach. The fitting curve matches the experimental curve very well. After deconvolution, the FTIR spectra region of 3800 to 3000 cm^{-1} was resolved into three or four bands. The absorbance of the band obtained from a local baseline fitting was automatically calculated at the maximum absorbance found by using the sensitivity of the PeakFit software.

Determination of cellulose crystallinity by X-ray diffraction (XRD)

The X-ray diffraction (XRD) scattering pattern of the pulp was analyzed on a Philipps X'Pert MPD diffractometer using a Cu-Kα source (λ = 0.154 nm) in the 2θ range of 4 to 60° and a scanning step width of 0.02°/scan. Each analysis was repeated in triplicate. The other scattering was subtracted from the pulp diffraction diagram. The crystalline reflections and amorphous halo were defined according to previously described recommendations (Wan *et al.* 2010 and Liao *et al.* 2011). The degree of cellulose crystallinity (%) and the average width of the crystal in (002) lattice plane were calculated as the following equation (Kim and Hotzapple 2006):

$$\mathrm{CrI} = \frac{I_{002} - I_{am}}{I_{002}} \times 100 \quad (1)$$

where I_{002} and I_{am} are the scattering intensities from the diffraction intensity of (002) plane and the diffraction intensity at 2θ=18°, respectively;

$$L_{002} = \frac{K\lambda}{\beta_\theta \cos\theta} \quad (2)$$

where β_θ is the width of the middle height of the (002) reflection; θ is the maximum of the (002) reflection, in radians; λ is the wave length of the X-ray source (0.154 nm); and K is the Scherrer constant (0.9).

The spectra were deconvolved using Gaussian mixed with Gaussian-Lorentzian profiles. After deconvolution, the several parameters can be calculated (He *et al.* 2007; Heinze and Liebert 2001), and the crystalline index and apparent crystallite size was obtained.

Sample preparation for CP/MAS ^{13}C NMR

The pulps for ^{13}C NMR analysis were subjected to a mild chlorite delignification with $NaClO_2$ (1.5 g / g sample) under acidic conditions at room temperature followed by treatment with 0.1 M NaOH overnight. Between the $NaClO_2$ and NaOH stages, the samples were rinsed with deionized water to pH 4-5. The overall procedure was repeated twice. Afterwards, the samples were then hydrolyzed for 8 h in 2.5 M HCl at 100 °C (Hult *et al.* 2001), and washed with deionized water to a pH of 4-5 prior to drying freely.

Determination of NMR spectroscopy

The spectra of all samples (water content 40 to 60% by weight) were recorded on a Bruker AVANCE AV 400 instrument (at ambient temperature) operating at 7.04 T for ^{13}C NMR. The pulp samples were packed in a zirconium oxide rotor. The MAS rate was 4-5 kHz. The CP/MAS ^{13}C NMR data was acquired with a CP pulse sequence using a 3.5 ms proton 90° pulse, 800 ms contact pulse, and a 2.5 s delay between repetitions.

RESULTS AND DISCUSSION

Changes of Functional Groups of Eucalyptus Cellulose Fibers during Beating

Infrared spectroscopy, which is known to be sensitive to certain structural features, has had a long tradition in wood research. The two information-rich regions of the FTIR spectra of the eucalyptus fibers were 3800 cm^{-1} to 2800 cm^{-1} and 1800 cm^{-1} to 600 cm^{-1}, as shown in Figs. 1 A and B, respectively. The absorption bands and the corresponding structure assignments for the infrared spectra were reported in previous articles (Wan *et al.* 2010; Chen *et al.* 2011; Poletto *et al.* 2011). Table 1 shows the absorption bands and the corresponding structure assignments from the infrared spectra. The band in the range of 1700 cm^{-1} to 1550 cm^{-1} may be associated with water absorption. The band in the range of 1430 cm^{-1} can be assigned to the HCH and OCH in-plane bending vibration, and 1365 cm^{-1} assigned as the in-plane CH bending may be from hemicellulose or cellulose, respectively.

Table 1. Infrared Spectra Adsorption and Structural Assignment

Wavenumber (cm^{-1})	Assignment
3350	Intra-molecular OH stretching vibration
2900	CH, CH_2 and intermolecular OH stretching vibration
1637	Adsorbed water and oxygen-containing group
1432	HCH and OCH in-plane bending vibration.
1372	Cellulose and hemicelluloses CH bending vibration
1163	Cellulose and hemicelluloses C-O-C stretching vibration
1058 -1060	Cellulose and hemicelluloses C=O stretching vibration
898	β- glycosidic bond vibration

Figure 1 shows the FTIR spectra of eucalyptus pulp. From top to bottom, the spectra are those for pulps that have been refined for 25 min, 15 min, and 5 min, respectively. Despite the absorbance intensity changes, wave number shifts are also shown for the bands at 1643→1654→1660 cm^{-1}, 2900→2898→2900 cm^{-1}, and 3406→3379→3436 cm^{-1} (higher wave number with lower absorbance), so in the region of the FTIR spectra, some bands exhibited little differences. Additionally, seen from these three samples in Fig. 1, a broad band can be observed at the 3600 cm^{-1} to 3200 cm^{-1} region, which was attributed to the stretching of the hydroxyl (OH) groups, at the 3000 cm^{-1} to 2800 cm^{-1} region, which was attributed to CH stretching (Dai and Fan 2011). From Fig. 1 it is seen that the CH_2 stretching vibration can split into two absorption peaks, which are symmetric stretching vibration and antisymmetric stretching vibration. However, in the above FTIR spectra, CH_2 stretching vibration appears as an absorption

peak at about 2900 cm^{-1}, which is due to the effect of hydrogen bonds after the CH_2OH group became aligned with the crystal lattice during beating. This resulted in the double peaks of symmetric and antisymmetric stretching vibration tending to a single peak between those for symmetric and antisymmetric stretching vibrations. Moreover, it is clear that in Fig. 1 the FTIR spectra show the absorption peak of the intra-molecular OH stretching vibration frequency changed with different beaten time. The shift to a different frequency suggests that the absorbance of the hydrogen bond strength was changed. However, the characteristic functional groups of the samples are essentially unchanged during beating, which suggested the composition was similar, because beating is just a physico-mechanical process.

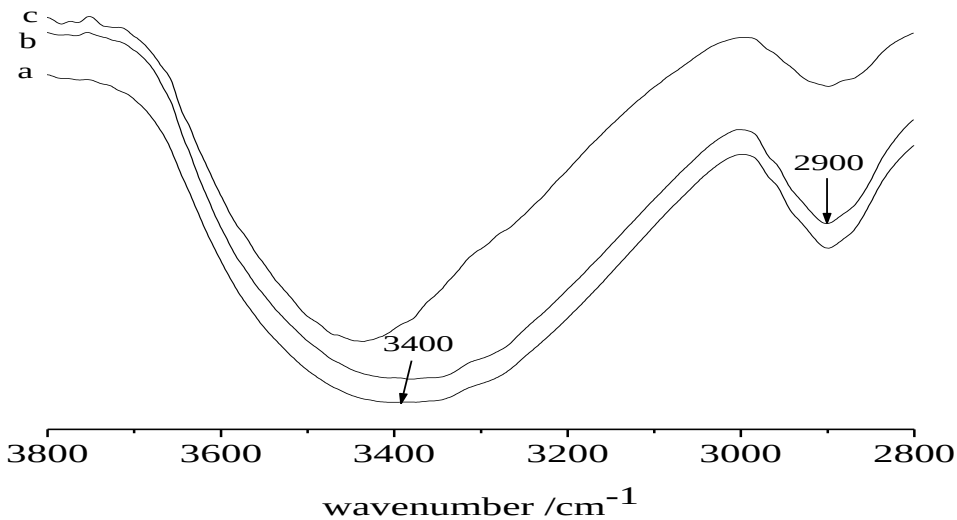

A

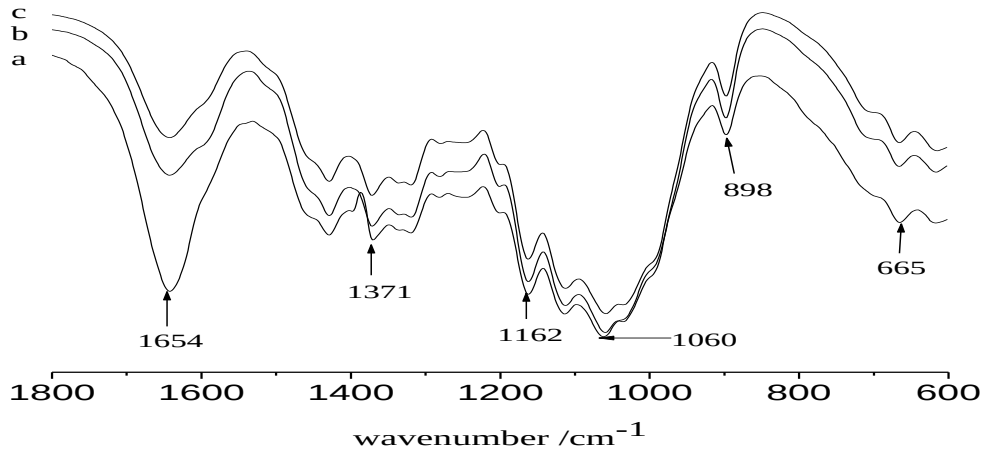

B

Fig. 1. FTIR spectra of the different beating time: (a) 5 min, (b) 15 min and (c) 25 min; spectra regions: **A**: 3800-2800 cm^{-1} and **B**: 1800-600 cm^{-1}

Content of Different Hydrogen Bond Models of Eucalyptus Fibers during Beating

Despite the small changes in the shifted hydrogen bonds that were found, the details about the content of different hydrogen bond models were still unobvious. Most research has focused on functional groups stretching, whereas limited research has focused on the details about the content of different hydrogen bond models of cellulose crystallinity. Since the use of infrared spectroscopy to elucidate molecular structures, much effort has been devoted to separating the overlapping bands deriving, for example, from hydrogen bonds (Oh *et al.* 2005). Fibers join together by forming hydrogen bonds, and the strength of the sheet can be correlated to the number of inter-fiber bonds formed. The large number of polar hydroxyl groups in cellulose chains make cellulose polymer chains predestined to form hydrogen bonds within the same polymer chain strain and with other polymer chain strands. In the generally accepted structure of cellulose I, intra-molecular hydrogen bonds of the types O(3)H···O(5) and O(2)H···O(6) and the inter-molecular hydrogen bonds for O(6)H···O(3′) were studied, respectively (Schwanninger *et al.* 2004). As a result of hydroxyl groups showing different polarities, cellulose has different crystalline structures. And the cellulose fiber structural changes through various recycle periods of eucalyptus fibers were studied by FTIR (Chen *et al.* 2012).

The transformed intensity spectrum obtained from eucalyptus fibers were analyzed by using the PeakFit software's Gaussian function (Maréchal and Chanzy 2000; Oh *et al.* 2005; Popescu *et al.* 2009) to differentiate the hydrogen bond types. Generally, the curve fitting of IR spectra can enhance the apparent resolution, and amplify small differences in the IR spectra. Figure 2 shows the FTIR spectra of the hydrogen-bonded O-H stretching vibrations with the corrected baseline. Assuming that all the vibration modes follow a Gaussian distribution, mixed modes of hydrogen-bonded O-H stretching can be resolved into three bands for native cellulose.

According to Fig. 2, there was much difference among the three samples; Table 2 quantifies the results of the FTIR spectra for the amounts of hydrogen bond O-H stretching vibrations (with the baseline correction). The total content of the intra-molecular hydrogen bond O(2)H···O(6) and O(3)H···O(5) decreased by 17.09%, and the content of inter-molecular O(6)H···O(3′) increased by 11.20% when the beating time increased from 5 to 15 min. This is due to the fact that there was breakage or generation of hydrogen bonds during beating (Mohkami and Talaeipour 2011). Beating exposes the interior of the fiber, increasing surface area and allowing a greater number of inter-fiber bonds to form, strengthening the sheet. However, the total content of the intra-molecular hydrogen bond increased by 16.06% and the content of inter-molecular O(6)H···O(3′) decreased by 33.66% when the time was increased from 15 to 25 min, compared with the sample beaten at 5 min. Since hemicelluloses have relatively short chain lengths and the prevalence of hydrogen bonds can provide valuable linkages between two cellulose fibers, they swell greatly and absorb a good quantity of water when wet; they are also the most easily degraded compound present in wood, especially in low-yield pulping. It is likely that the beating operation affects the internal and the external surface chemical composition of the fibers, and the majority of hemicelluloses are often lost in low yield pulping with increasing beating time, which results in the decrease in the content of inter-molecular hydrogen bonding with 5 min of beating. In addition, the inter-molecular hydrogen bonding of cellulose is dominant, and it manifests itself as a force between fibers to combine the chains of cellulose, while intra-molecular hydrogen is just in

position within the auxiliary. The phenomenon is also in accordance with the regular pattern of the energy of hydrogen bonds (Struszczyk *et al.* 1986).

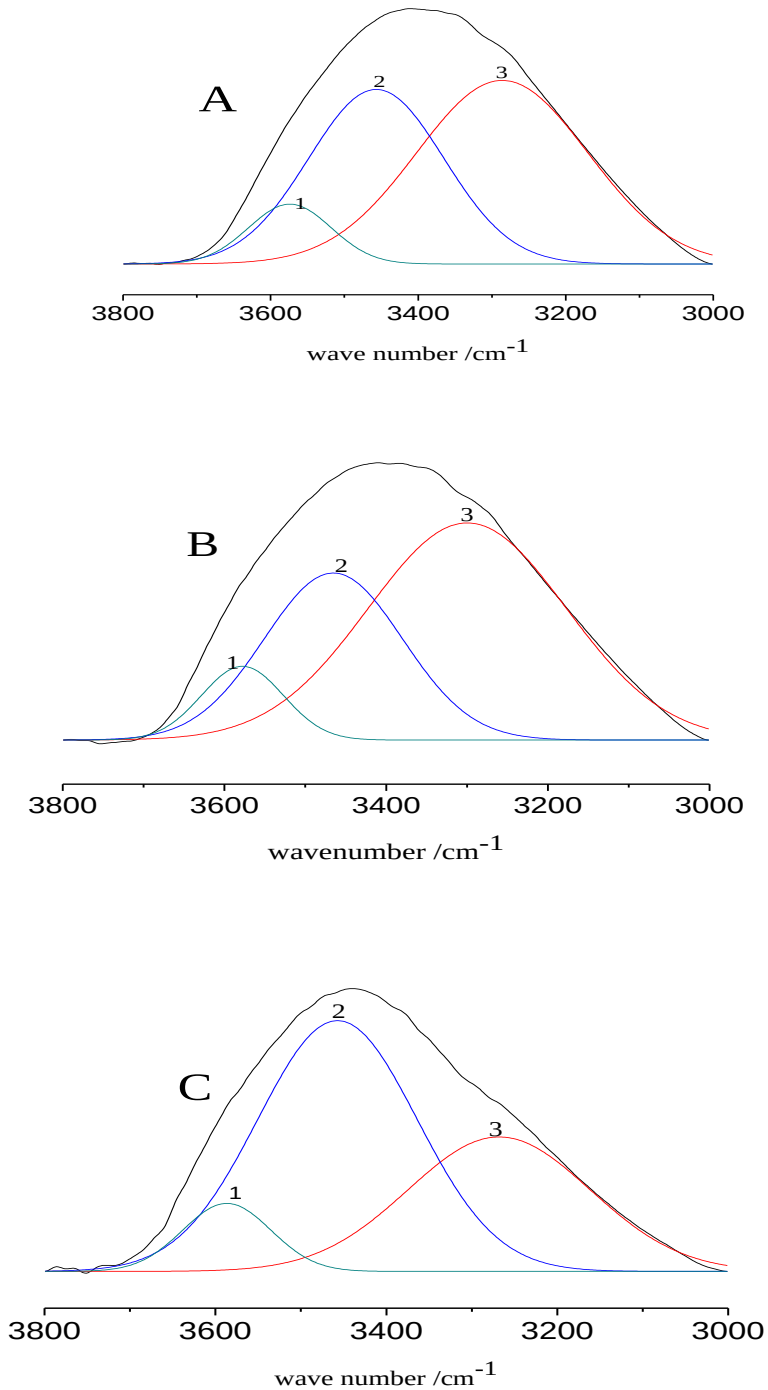

Fig. 2. Spectra fitting of hydrogen bond region of FTIR spectrum of eucalyptus fibers with different beating time: (**A**) 5 min, (**B**) 15 min and (**C**) 25 min; bonding modes: (1) intra-molecular hydrogen bond O(2)H···O(6); (2) intra-molecular hydrogen bond O(3)H···O(5); and (3) inter-molecular hydrogen bond O(6)H···O(3′).

Table 2. The Content of Different Hydrogen Bond Forms Obtained by FTIR Gaussian Fitting

Beating Time (min.)	Hydrogen bond	Wave number (cm^{-1})	Content (%)
5	O(2)H···O(6)	3573	8.25
	O(3)H···O(5)	3456	39.33
	O(6)H···O(3′)	3286	52.43
15	O(2)H···O(6)	3577	8.18
	O(3)H···O(5)	3465	31.27
	O(6)H···O(3′)	3299	58.30
25	O(2)H···O(6)	3586	8.52
	O(3)H···O(5)	3457	56.70
	O(6)H···O(3′)	3268	34.78

Crystal Type of Eucalyptus Fibers by Using X-Ray Diffraction (XRD) during Beating

The XRD spectra of the eucalyptus fibers are shown in Fig. 3. As can been seen, the eucalyptus fiber peaks of X-ray diffraction curve is typical crystal diffraction of cellulose I. The results indicated that the ($10\bar{1}$) and (101) faces overlap, and the diffraction angle about the (002) lattice plane differ by a small amount, which suggests that cooking process may destroy the crystalline structure of cellulose. However, the phenomenon shows that the cellulose crystal type (cellulose I) did not change.

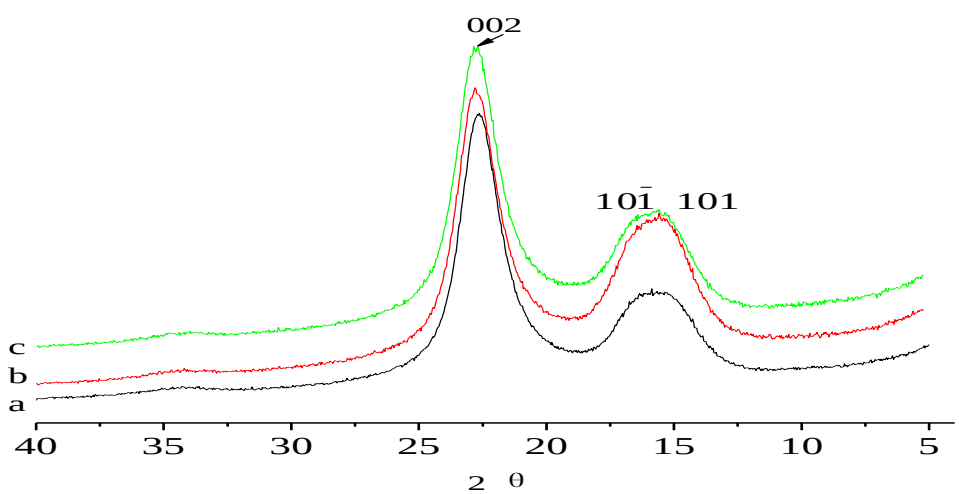

Fig. 3. XRD spectra of eucalyptus fibers with different beating time: (a) 5 min, (b) 15 min, and (c) 25 min.

Microcrystalline Structure and Properties

The crystallinity of eucalyptus fibers in treated samples with different beating times were analyzed by X-ray diffraction (XRD). This method is based on the height of the diffraction peak (Segal *et al.* 1962). When the beating time was 5, 15, and 25 min, the crystallinity of the eucalyptus wood pulp samples was 80.62%, 76.30%, and 77.06%,

respectively. The information obtained shows that the relative height to the minimum can only be taken as a rough approximation of the contribution of amorphous cellulose to the cellulose diffraction spectrum (Mohkami and Talaeipour 2011). However, the precision and accuracy of diffraction peak positions resolved from the spectra by means of the residuals fitting procedure was investigated for their accuracy. In order to examine the intensities of diffraction bands and to establish the crystalline and the amorphous areas more precisely, the diffractograms were deconvoluted as shown in Fig. 4. The positions of the peaks responsible for the cellulose crystalline form I were found to be significantly different in the three eucalyptus pulps with different beating time.

After deconvolution, five bands were observed, namely: the 14.5° (2θ) reflection assigned to the (101) crystallographic plane, the 16.5° (2θ) reflection, assigned to the $(10\bar{1})$ crystallographic plane, the 18.0° (2θ) reflection, assigned to amorphous phases, and the 22.4° (2θ) reflection, assigned to the (002) or (200) crystallographic planes of cellulose I (Colom *et al.* 2003; Marcovich *et al.* 2001). The crystallinity obtained by peak area X-ray analysis is in accordance with that found by the strength of the peak (Chen *et al.* 2004). The function which calculates mean cross sectional area (A) is given by: $A = L_{002} \times 1/2(L_{10\bar{1}} + L_{101})$ (where L_{002}, $L_{10\bar{1}}$ and L_{101} are the average width of crystal in (002), $(10\bar{1})$, and (101), respectively) (Hult *et al.* 2003). Crystallinity was calculated from the ratio of the area of all crystalline peaks to the total area.

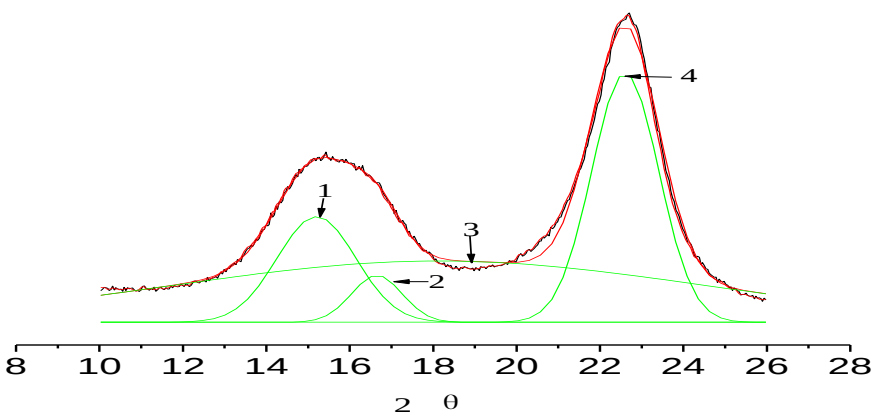

Fig. 4. Deconvoluted XRD spectra of eucalyptus cellulose fibers: 1 (101) crystallographic plane, 2 $(10\bar{1})$ crystallographic plane, 3 amorphous phase, and 4 (002) crystallographic plane

Crucial for the analysis of the XRD data is the separation of the reflection (002) from the amorphous background and reflections of (101) and $(10\bar{1})$; these peaks are separated by Gaussian deconvolution. During refining the eucalyptus fibers suffer shear and frictional forces, giving rise to internal delamination and fibrillation at the fiber surfaces. Such effects result in better conformability of the fibers. The presence of fibrils resulting from beating, along with the generation of fines and delamination between the fiber layers, such as the primary and secondary wall, imply changes in the hydrogen bonded structure, changing the crystallinity (Carvalho *et al.* 2005). In Table 3, the calculated parameters from X-ray diffractogram for the studied samples are presented.

Table 3. Analyses of Cellulose Super-Molecular Structure in Eucalyptus Kraft Pulps with Different Beating Time

Beating time (min)	Lattice plane (nm)	Diffraction angle 2θ (°)	L_{hkl} (nm)	CrI (%)	A (nm^2)
	$10\bar{1}$	15.17	5.3		
5	101	16.25	6.7	76.0	31.25
	002	22.85	5.5		
	$10\bar{1}$	15.4	4.2		
15	101	16.42	7.2	68.9	23.84
	002	22.87	5.2		
	$10\bar{1}$	15.23	4.6		
25	101	16.61	6.8	70.2	25.93
	002	22.64	5.4		

The average width of crystal plane and the cross-sectional area of eucalyptus cellulose fibers have been analyzed (Wan *et al.* 2010). Table 3 shows the X-ray spectra of the eucalyptus fibers at different beating time. Changes in cellulose super-molecular structure of eucalyptus pulps were analyzed. The average width of diffraction peaks for (002), ($10\bar{1}$), and (101) lattice planes decreased as the beating time ranged from 5 to 15 min, but when the time was extended to 25 min, the average width of lattice plane increased. The changes about the average width of crystallite in (002), ($10\bar{1}$), and (101) planes exhibited the same tendency as the increase of beating time. The mean cross sectional area of the three samples changed, influencing the accessibility and homogeneity of the fibers. The present results correspond with the conclusion of native cellulose, which has been reported (Hermans and Weidinger 2003). It is likely that the increase in surface area exposes a greater number of the fibers' internal pores, allowing for more water retention initially but also causing a greater observed degree of hornification. This indicates that beating may play a role on cellulose structural changes. This also confirms the positive effect of beating in limiting the degree of cellulose hornification.

Content of Polymorphs of the Eucalyptus Cellulose by ^{13}C NMR Spectra during Beating

The NMR spectra of the eucalyptus pulp samples are shown in Fig. 5. The signals assigned to C4 were partly separated into two clusters, labeled *i* and *s*, which were assigned to the interiors and surfaces of the crystalline domains, respectively. Poorly resolved splitting within the cluster labeled *i* was attributed to the presence of both the I_α and I_β domains together with para-crystalline cellulose forms. Partly resolved splitting in the cluster labeled *s* might be associated with the non-crystalline area. Only subtle differences in spectral details can be observed between the three eucalyptus pulp samples.

Recently, a large amount of information about cellulose I_α and cellulose I_β has become available, and it is clear that the two forms differ in hydrogen bonding (Sugiyama *et al.* 1991); however, the precise content cannot been obtained during beating. A method for quantifying the states of order found within cellulose I has been proposed based on CP/MAS ^{13}C NMR in combination with spectral fitting (Hult 2001; Newman 2004). This approach has been used by others to assess the cellulose crystallinity (Horii *et al*. 1987; Hult *et al*. 2002).

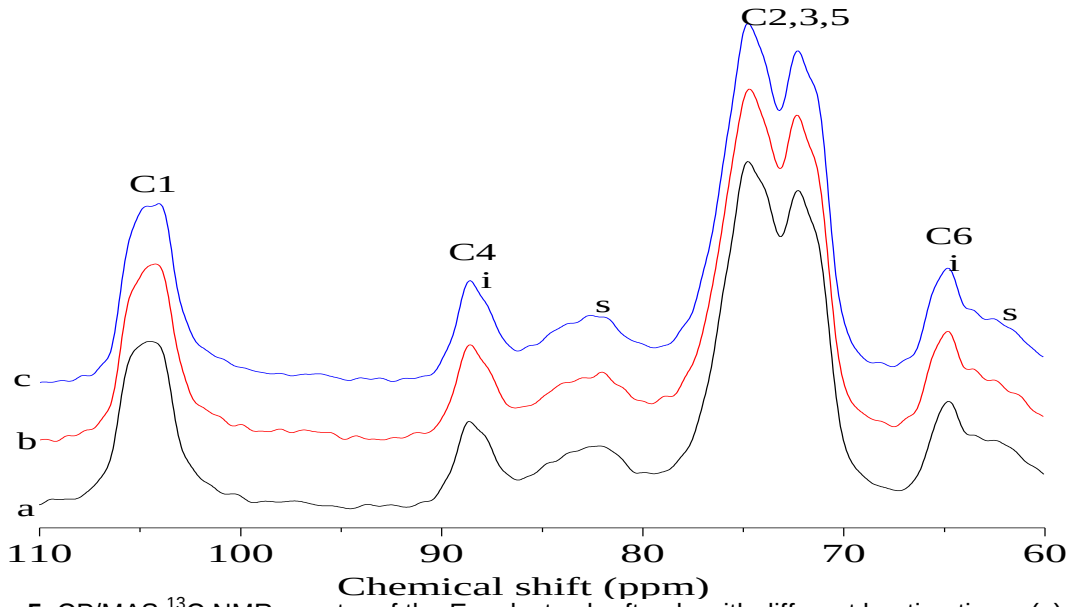

Fig. 5. CP/MAS ^{13}C NMR spectra of the Eucalyptus kraft pulp with different beating time: (a) 5 min, (b) 15 min, and (c) 25 min

Lorentzian and Gaussian functions were used to perform the deconvolution of the C4 peaks. A combination of Lorentzian and Gaussian functions was used to fit the C4 region (80 to 92 ppm) with seven peaks in that range (Wan 2010; Chen 2010; Newman 2004). The peak assigned to more ordered cellulose structures includes those peaks previously assigned to the I_α, I_β, and para-crystalline cellulose components (see Fig. 6).

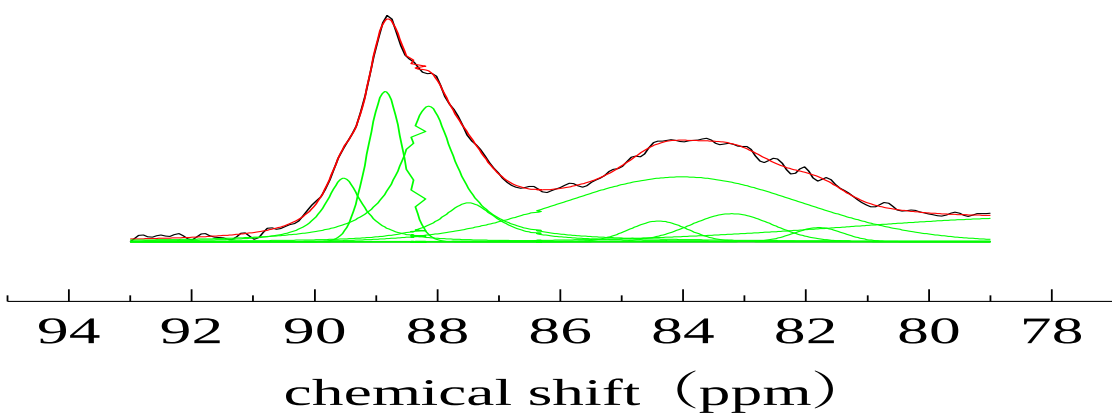

Fig. 6. Lorentzian and Gaussian line shape-fitting of the C-4 spectral region of eucalyptus fibers

The results of the spectral fitting for the cellulose C4 region of the ^{13}C NMR spectra of the pulps with different beating times are shown in Fig. 6 and Table 4. It is apparent that the different cellulose polymorphs are usually analyzed on the basis of the form of the C4 signal. During the beating process the content of different cellulose polymorphs were obtained. There were little changes in the content of cellulose I_α and cellulose I_β, but the content of the cellulose I_β in the three samples was observed to be substantially higher than cellulose I_α.

Table 4. Results of Spectral Fitting for the C4 Region of CP/MAS ^{13}C NMR Spectrum, Cellulose I_{α}, Cellulose $I_{\alpha+\beta}$Cellulose I_{β} , CrI with Different Beating Time

Beating time (min.)	5	15	25
Cellulose I_{α} (%) 88.8 ppm	4.18	4.01	4.23
Cellulose $I_{\alpha+\beta}$ (%) 88.7 ppm	1.4	3.4	2.8
Cellulose I_{β} (%) 86.7 ppm	34.8	29.5	33.2
Para-crystalline cellulose(%) 87.9 ppm	19.2	18.3	20.1
CrI (%)	61	57	60

Results are in complete agreement with I_{α} cellulose which has been reported to be the dominant polymorph in bacterial and algal celluloses, while I_{β} cellulose is predominant in higher plants such as cotton and wood (Sun *et al*. 2004). Temperature is well controlled, and it is the most important factor among the parameters which seem to influence the transformation between I_{α} and I_{β} (Debzi *et al.* 1991; Popescu *et al*. 2007). It could be expected that para-crystalline cellulose was converted into the more stable cellulose I_{β}, not the cellulose I_{α}. And the replacement of cellulose-water interactions by cellulose-cellulose interactions may affect the cellulose structure and dynamics of the cellulose hydrogen bonds at the fibril surfaces, resulting in the changes in the content of the polymorphs of the eucalyptus cellulose. However, this may be a very inconspicuous change. The crystallinity of the cellulose decreased when the beating time ranged from 5 to 15 min. This demonstrates that the special structure of PFI refining plate induces an "external effect" on the fibers (Liu *et al.* 2002), and this hardens the fiber surfaces and the partly activates the cellulose. However, the crystallinity increased slowly when the beating ranged from 15 to 25 min. The reason was that more hydroxyl groups are fractionated out with further beating (Bhardwaj *et al*. 2007), which results in the adsorption of free water by fiber. Subsequently, during the drying or paper, water evaporates from the voids of cell walls, leading to the irreversible collapse of the cell wall. Hence, the crystallinity increased. As can been seen, the changes of the crystallinity during beating obtained by ^{13}C NMR were in full agreement with the results obtained by X-ray diffraction. It can be concluded that the pulp's ability to form fiber-fiber hydrogen bonds is regenerated to some extent during beating.

Changes of Crystal Size of Eucalyptus Fibers during Beating

The average lateral fibril and lateral fibril aggregate dimensions are calculated from quantitative spectra of pure cellulose isolated from the kraft pulps (Hult *et al.* 2000; Wickholm *et al.* 1998).

In Table 5, it is apparent that the average fibril sizes and fibril aggregate sizes are also given for the three samples; the average fibril size was relatively constant between 5.18 and 4.6 nm for the three samples, which exhibited no major differences. However, the cellulose fibril size calculated by the NMR method was lower than that obtained by X-ray Diffraction. For example, when the beating time was 5 min, the CP/MAS ^{13}C NMR estimates gave a lateral fibril dimension of 5.18 nm, but the average width of crystallites

in 002 (lateral fibril dimension) was 5.5 nm. The probable reason for the difference was that only material within the crystallites appears as crystalline in NMR spectra; therefore the NMR crystallite size depends on crystalline perfection (Maunu *et al*. 2000). However, the fibrils aggregate size ranges from 22.2 nm to 27.8 nm. The only significant difference is the change of the fibrils aggregate dimensions.

Table 5. The Results of Spectral Fitting for the C4 Region of CP/MAS ^{13}C NMR Spectrum, Accessible Fibril Surfaces, Inaccessible Fibril Surfaces, Lateral Fibril Dimension, and Fibrils Aggregate Size with Different Beating Times

Beating time (min)	**5**	**15**	**25**
Accessible fibril surfaces (%) 84.09 ppm , 81.43 ppm	9	10	8
Inaccessible fibril surfaces (%) 83.18 ppm	30	33	32
Lateral fibrils size (nm)	5.18	4.6	5.0
Lateral fibrils aggregate size (nm)	24.7	22.2	27.8

As a result of beating, the fiber wall is fractured and some of the surface material is removed, exposing more hydroxyl groups. Thus, beating increases the interaction between fiber and water, and it results in more microfibrils (Nishiyama *et al.* 2002). This allows for increased swelling of the fiber during beating, and it can lead to further fibril aggregation during papermaking (Hult *et al.* 2001).

CONCLUSIONS

This work presents an attempt to explain the influence of beating time on the content of hydrogen bonds corresponding to different models. Also, it was shown that beating affects the crystallinity of eucalyptus pulp fibers, as well as the different cellulose polymorphs. Pulps with different beating time differed greatly in structure. By increasing the beating time, both the content of different hydrogen bonds and the crystallinity were affected. Accordingly, greater changes occurred in the average fibril aggregate size and cellulose crystalline types. Cellulose crystallinity decreased and then increased with an increase in beating time. The average fibril sizes and fibril aggregate sizes of unbleached eucalyptus fibers increased with the increase in crystallinity. In confronting the characteristics of fibers recreated during beating, it appears that the mechanical action of beating can modify fiber ultra-structural integrity in a way that should potentially improve final paper properties and does not cause extreme damage in the fiber.

ACKNOWLEDGMENTS

This work was supported by The National Natural Science Foundation of China (No.31170551) and (No. 31200458), Ph.D.Program Foundation of Minstry of Education of China (No.20110172110015).

REFERENCES CITED

Baratieri, M., Baggio, P., Fiori, L., and Grigiante, M. (2008). "Biomass as an energy source: Thermodynamic constraints on the performance of the conversion process," *Bioresource Technology* 99(15), 7063-7073.

Bhardwaj, N. K., Hoang, V., and Nguyen, K. L. (2007). "A comparative study of the effect of refining on physical and electrokinetic properties of various cellulosic fibres," *Bioresource Technology* 98(8), 1647-1654.

Billosta, V., Brandstrom, J., Cochaux, A., Joseleau, J. P. and Ruel, K. (2006). "Ultrastructural organization of wood cell wall may explain some modifications undergone by fibres during pulping process," *Cell. Chem. Technol.* 40, 231-237.

Chen, Y. M., Wan, J. Q., Zhang, X. L. (2012). "Effect of beating on recycled properties of unbleached eucalyptus cellulose fiber," *Carbohydrate Polymers* 87(1), 730-736.

Chen, Y. M., Wan, J. Q., Ma, Y. W. (2010). "Effect of noncellulosic constituents on physical properties and pore structure of recycled fiber," *Appita Journal* 62(4), 290-295.

Carvalho, M., G., Santos, J. M. R. C. A., Martins, A. A., and Figueiredo, M. M. (2005). "The effects of beating, web forming and sizing on the surface energy of *Eucalyptus globulus* kraft fibers evaluated by inverse gas chromatography," *Cellulose* 12(4), 371-383.

Chen, R., Jakes, K. A., Foreman, D. W. (2004). "Peak-fitting analysis of cotton fiber powder X-ray diffraction spectra," *Journal of Applied Polymer Science* 93(5), 2019-2024

Colom, X., Carrillo, F., Nogues, F., and Garriga, P. (2003). "Structural analysis of photodegraded wood by means of FTIR spectroscopy," *Polymer Degradation and Stability* 80(3), 543-549.

Debzi, E. M., Chanzy, H., Sugiyama, J., Tekely, P., and Excoffier, G. (1991). "The $I_\alpha \rightarrow I_\beta$ transformation of highly crystalline cellulose by anneaing in various mediums," *Macromolecules* 24(26), 6816-6822.

Duchesne, I., Hult, E. L., Molin, U., Daniel, G., Iversen, T., and Lennhon H. (2001). "The influence of hemicellulose on fibril-aggregation of kraft pulp fibers as revealed by FE-SEM and CP/MAS 13C NMR," *Cellulose* 8(2), 103-111.

Dai, D. S., and Fan, M. Z. (2011). "Investigation of the dislocation of natural fibres by Fourier transform infrared spectroscopy," *Vibrational Spectroscopy* 55(2), 300-306.

Gümüskaya, E., Usta, M., and Kirei, H. (2003). "The effects of various pulping conditions oncrystalline structure of cellulose in cotton linters," *Polym. Degrad. Stab.* 81(3), 559-64.

He, J., Tang, Y., and Wang, S. Y. (2007). "Differences in morphological characteristics of bamboo fibers and other natural cellulose fibers: Studies on X-ray diffraction, solid

state 13C-CP/MAS NMR, and second derivative FTIR spectroscopy data," *Iranian Polymer Journal* 16(12), 807-818.

Hermans, P. H., and Weidinger, A. (2003). "X-ray studies on the crystallinity of cellulose," *Journal of Polymer Science* 4(2), 135-144.

Hult, E. L., Iversen, T., and Sugiyama, J. (2003). "Characterization of the supermolecular structure of cellulose in wood pulp fibers," *Cellulose* 10(2), 103-110.

Hult, E. L., Liitiä, T., Maunu, S., L., Hortling, B., and Iversen, T. (2002). "A CP/MAS 13C-NMR study of cellulose structure on the surface of refined kraft pulp fibers," *Carbohydrate Polymers* 49(2), 231-234

Hult, E. L., Larsson, P. T., and Iversen, T. (2001). "Cellulose fibril aggregation – An inherent property of kraft pulps," *Polymer* 42 (8), 3309-3314.

Heinze, T., and Liebert, T. (2001). "Unconventional methods in cellulose functionalization," *Progress in Polymer Science* 26(9), 1689-1762.

Horii, F., Hiral, A., and Kitamaru, R. (1987). "CP/MAS ^{13}C NMR spectra of the crystalline components of native cellulose," *Macromlecules* 20(9), 2117-2120.

Jiménez, L., López, F., and Alaejos, J. (2006). "Materias primas alternativas para pastas depapel. Tipos, características, procesosy situación mundial," *Ingeniería Química* 435(4), 76-90.

Ibrahem, A. A., Yousef, M. A., and EL-Meadwy, S. A. (1989). "Effect of beating on fiber crystallinity and physical properties of paper sheets," *Journal of Islamic Academy of Sciences* 2(4), 295-298.

Kim, S., and Holtzapple, M. T. (2006). "Effect of structural features on enzyme digestibility of corn stover," *Bioresource Technology* 97(4), 583-591.

Kure, K. A. and Dahlqvit, G. (1998). "Development of structural fiber properties in high intensity refining," *Pulp Paper Can*. 99(7), 59-63.

Lorenzo, M. L., Nierstrasz, V. A., and Warmoeskerken, M. M. C. G. (2009). "Endoxylanase action towards the improvement of recycled fiber properties," *Cellulose* 16(1), 103-115.

Liao, Z. D., Huang, Z. Q., Hu, H. Y., Zhang, Y. J., and Tan, Y. F. (2011). "Microscopic structure and properties changes of cassava stillage residue pretreated by mechanical activation," *Bioresource Technology* 102(17), 7953-7958.

Liu, D. T., Li, J., Yang, R. D., Mo, L. H., Huang, L. H., Chen, Q. F., and Chen, K. F. (2008). "Preparation and characteristics of moulded biodegradable cellulose fibers/MPU-20 composites (CFMCS) by steam injection technology," *Carbohydrate Polymers* 74(2), 290-300.

Liu, R., Yu, H., and Huang, Y. (2005). "Structure and morphology of cellulose in wheat straw," *Cellulose* 12(1), 25-34.

Liu, S. L., Li, G. S., Lei, L. R., Cao, G. P., and Li, S. Y. (2002). "Optimum treatment of waste pulp using medium consistency pulp refining," *China Pulp and Paper Industry* 23(10), 38-39.

Miyamoto, H., Ago, M., Yamane, C., Seguchi, M., and Ueda, K. (2011). "Supermolecular structure of cellulose/amylose blends prepared from aqueous NaOH solutions and effects of amylose on structural formation of cellulose from its solution," *Carbohydrate Research* 346(6), 807-814.

Mohkami, M., and Talaeipour, M. (2011). "Investigation of the chemical structure of carboxylated and carboxymethlated fibersfrom waste paper via XRD and FTIR analysis," *BioResources* 6(2), 1988-2003.

Marcovich, N. E., Reboredo, M. M., and Aranguren, M. I. (2001). "Modified wood flour as thermoset fillers. II. Thermal degradation of wood flours and composites," *Thermochimica Acta* 372(1-2), 45-57.

Maunu, S., Liitiä, T., Kauliomäki, S., Hortling, B., Sundquist, J. (2000). "^{13}C CPMAS NMR investigations of cellulose polymorphs in different pulps," *Cellulose* 7(2), 147-159.

Maréchal, Y., and Chanzy, H. (2000). "The hydrogen bond network in $I_ß$ cellulose as observed by infrared spectrometry," *Journal of Molecular Structure* 523(1-3), 183-196.

Newman, R. H. (2004). "Carbon-13 NMR evidence for cocrystallization of cellulose as a mechanism for hornification of bleached kraft pulp," *Cellulose* 11(1), 45-52.

Oh, S. Y., Yoo, D. Il., Shinet, Y., Kim, C. H., Kim, H. Y., Chung, Y. S., Park, W. H., and Youk, J. H. (2005). "Crystallines tructure analysis of cellulose treated with sodium Hydroxide and carbon dioxide by means of X-ray diffraction and FTIR spectroscopy," *Carbohydrate Research* 340(15), 2376-2391.

Poletto, M., Pistor, V., Zeni, M., and Zattera, A. J. (2011). "Crystalline properties and decomposition kinetics of cellulose fibers in wood pulp obtained by two pulping processes," *Polymer Degradation and Stability* 96(4), 679-685.

Popescu, C. M., Singurel, G., Popescu, M. C., Vasile, C., Argyropoulos, D., and Willför, S. (2009). "Vibrational spectroscopy and X-ray diffraction methods to establish the differences between hardwood and softwood," *Carbohydrate Polymers* 77(4), 851-857.

Popescu, C. M., Popescu, M. C., Singurel, G., Vasile, C., Argyropoulos, D. S., and Willfor, S. (2007). "Spectral characterization of eucalyptus wood," *Applied Spectroscopy* 61(11), 1168-1177

Ruel, K., Barnoud, F., and Goring, D. A. I. (1978). "Lamellation in the S_2 layer of softwood tracheids as demonstrated by scanning transmission electron microscopy," *Wood Sci. Technol*.12(4), 287-291.

Schwanninger, M., Rodrigues, J. C., Pereira, H., and Hinterstoisser, B. (2004). "Effects of short-time vibratory ball milling on the shape of FT-IR spectra of wood and cellulose," *Vibrational Spectroscopy* 36(1), 23-40.

Struszczyk, H. (1986). "Modification of lignins. Ⅲ. Reaction of lignosulfonates with chlorophosphazenes," *Journal of Macromolecular Science* A23(8), 973-992.

Segal, L., Creely, J. J., Martin, A. E. J., and Conrad, C. M. (1962). "An empirical method for estimating the degree of crystallinity of native cellulose using the X-ray diffractometer," *Tex. Res. J.* 29(10), 786-794.

Sodhi, N. S., Koh, L. P., and Clements, R. (2010). "Conserving Southeast Asian forest biodiversity in human-modified landscapes," *Biological Conservation* 143(10), 2375-2384.

Sun, J. X., Sun, X. F., Zhao, H., and Sun, R. C. (2004). "Isolation and characterization of cellulose from sugarcane bagasse," *Polymer Degradation and Stability* 84(2), 331-339.

Sugiyama, J., Persson, J., and Chanzy, H. (1991). "Combined infrared and electron diffraction study of the polymorphism of native cellulose," *Macromolecules* 24(9), 2461-2466.

Wan, J. Q., Wang, Y., Xiao, Q. (2010). "Effects of hemicellulose removal on cellulose fiber structure and recycling characteristics of eucalyptus pulp," *Bioresource Technology* 101(12), 4577-4583

Wan, J. Q., and Ma, Y. W. (2004). *Waste Papermaking and Pollution Control*, China Light Industry Press, Beijing.

Wickholm, K., Larsson, P. T., and Iversen, T. (1998). "Assignment of non-crystalline forms in cellulose I by CP/MAS 13C NMR spectroscopy," *Carbohydr. Res.* 312(3), 123-129.

Zhai, D. L., Cannon, C. H., and Slik, J. W. F. (2012). "Rubber and pulp plantations represent a double threat to Hainan's natural tropical forests," *Journal of Environment Management* 96(1), 64-73.

Article submitted: July 5, 2012; Peer review completed: September 29, 2012; Revised version received: October 14, 2012; Accepted: October 15, 2012; Published: December 14, 2012.